A Note on the Deficiency of NCEP/NCAR Reanalysis Surface Winds over the Equatorial Indian Ocean

B. N. Goswami and D. Sengupta
Centre for Atmospheric and Oceanic Sciences
Indian Institute of Science
Bangalore-560 012

Abstract

The seasonal cycle and intraseasonal variability of the National Centers for Environmental Prediction/ National Center for Atmospheric Research (NCEP) reanalysis surface winds over the Indian Ocean (IO) are assessed by comparing them with in situ surface observations from two moored buoys and winds from the SeaWinds scatterometer on the QuikSCAT satellite. The buoys are located in the central Bay of Bengal and eastern Arabian Sea. Both QuikSCAT and NCEP wind products reproduce closely the seasonal cycle and intraseasonal variability (10-60 day) in the *in situ* observations. In the equatorial IO, however, the seasonal mean NCEP windspeeds can be 2-3 m s^{-1} smaller and the amplitude of intraseasonal variability only about half that of QuikSCAT winds. The systematic errors of NCEP zonal winds are comparable to the annual mean or amplitude of the seasonal cycle in the equatorial IO. It is suggested that the systematic error of mean and intraseasonal variability of reanalysis winds is related to systematic error in the NCEP analysis of precipitation.

1. Introduction

The annual mean zonal wind in the equatorial Indian Ocean (IO) is rather small (about 1.5 m s^{-1} averaged between 40^{O}E-100^{O}E, 2^{O}S-2^{O}N) while the amplitude of the annual and semiannual components is about 2 m s^{-1}. The zonal wind stress drives eastward equatorial jets in the upper ocean in spring and fall (Wyrtki, 1973), contributes to the maintenance of warm SST in the eastern IO and influences the seasonal cycle of circulation in the Bay of Bengal (McCreary et al.1993, Vinayachandran et al. 1996) via coastal Kelvin waves. The interannual variations of the jets determine interannual changes in equatorial IO circulation and ocean temperature associated with the dipole mode (Saji et al. 1999, Murtugudde et al. 2000). The equatorial IO winds also have

vigorous intraseasonal oscillations (ISO) with periods between 10 to 20 days and 30 to 60 days (e.g. Webster et al. 1998, Goswami and Ajaya Mohan 2001). The amplitude of wind ISO in the equatorial IO could be as large as the seasonal variations (see Goswami et al., 1998, Sengupta et al., 2001). It might be expected that ISO of equatorial winds would influence the equatorial jets and Rossby waves and force new intraseasonal modes of upper ocean circulation. Therefore, reliable high frequency surface winds in the equatorial IO are necessary not only to understand the intraseasonal variability but also the seasonal and interannual variations of IO circulation.

The vast majority of model studies of the IO circulation (McCreary et al. , 1993, Murtugudde et al., 1998, 1999, 2000, Vinayachandran et al. 1996, Schiller et al.,1998) use monthly mean surface winds to study the seasonal cycle and interannual variability. The availability of global high frequency reanalysis wind products represented a step forward in the study of ISO. Recent studies (Sengupta et al. 2001, Han et al. 2001) using high frequency NCEP surface winds have begun to document a variety of circulation ISO in the tropical IO. Confidence in the results of these studies depends on reliability of the wind product used. The objective of this study is to examine the daily averaged surface wind from NCEP reanalysis (hereafter referred to as NRA) for its fidelity in representing the seasonal cycle and intraseasonal variability in the IO in general and the equatorial IO in particular.

The voluntary observing ship (VOS) data on surface winds are available with monthly resolution (e.g. Da Silva et al. 1994). However, poor sampling does not allow one to construct wind field with high temporal resolution from this source. Reanalysis products from the National Centers for Environmental Prediction/ National Center for Atmospheric Research (Kalnay et al, 1996) provide six hourly surface wind fields going back several decades while the ECMWF reanalysis (ERA, Gibson et al. 1997) provides similar data for about 15 years. The NCEP reanalysis has been widely used because it is easily available. The strength of reanalysis products is that they provide gridded data with global coverage at high temporal resolution, while a possible weakness is that systematic errors of the assimilation model influence the analysis in data sparse regions. Most atmospheric general circulation models (AGCMs) have significant systematic errors in simulating the strength and annual march of the tropical rain band, especially in the Indian monsoon region (Saji and Goswami, 1997, Gadgil and Sajani, 1998). Since the surface winds over the tropical oceans are primarily driven by tropospheric heating associated with deep convection, model biases in simulating precipitation may significantly influence surface wind analyses over data sparse regions such as the equatorial Indian Ocean (Saji and Goswami, 1997).

Like reanalysis, scatterometer vector winds have become available during the past decade (Liu 2002). The European Space Agency's European Remote Sensing Satellite (ERS-1/2) scatterometers measured both wind speed and direction but the areal coverage was poor due to the relatively narrow swath. The NASA scatterometer NSCAT (Naderi et al. 1991) operated for about ten months and provided high quality wind data over the oceans. The SeaWinds scatterometer on QuikSCAT satellite provides daily wind vectors from July 19, 1999 till present. The areal coverage of the wide swath SeaWinds scatterometer is 40% greater than that of NSCAT and 3.2 times greater than that of ERS.

Though the available record of QuikSCAT winds is not long, it has advantages over the other satellite derived products as it provides higher resolution both in space and time

High quality in situ measurement of winds with high temporal resolution can also be obtained from surface observations from moored buoys. Since 1998, the Department of Ocean Development (DOD) of India has maintained a set of moored buoys in the north Indian Ocean for routine monitoring of near surface meteorological and oceanographic conditions. As this data is available only at a few points in space they are mainly useful for validating other wind products.

In the present study, we compare the NRA surface winds with two independent sets of wind observations. We first carry out a limited comparison between available wind measurements from the buoys and both NRA and QuikSCAT winds, followed by a comparison of NRA and QuikSCAT wind fields in the tropical IO. A detailed validation of either QuikSCAT or NRA winds is not the objective of this study. In section 2 we describe the data used in this study. The annual cycle and intraseasonal variability of NRA surface winds are compared to those of QuikSCAT winds in Section 3. Although QuikSCAT winds are also another estimate of the true winds, previous validation studies (e.g. Chelton et al. 2001) have shown that the mean as well as the root mean square (rms) difference of QuikSCAT winds with respect to *in situ* observations are less than 1.0 m s^{-1}. Therefore, we take QuikSCAT as representative of observations. The possible cause for the differences between NRA and QuikSCAT products is also investigated and discussed in Section 4. The results are summarized in Section 5.

2.0 Data Used

The study uses daily averaged zonal (U) and meridional (V) winds at 10m height derived from NCEP reanalysis for the period 1999 to 2001. We obtained 'daily' fields from NCEP that are daily averages of the six hourly analyses. The NRA uses a frozen data assimilation system, the Global Data Assimilation System, (GDAS) and an observation base as complete as possible (Kalnay et al., 1996). The project involves recovery of land surface, ship, buoy, rawinsonde, satellite and other data and assimilating them using GDAS that is kept unchanged over the reanalysis period, 1948 to present. The GDAS includes a weather prediction model with horizontal resolution of T62; the Gaussian grid for the reanalysis winds is equivalent to approximately 210 km horizontal resolution. Use of a frozen data assimilation system (including the atmospheric model) throughout the reanalysis period largely eliminates nonstationary biases. The NRA surface winds are considered type B data (Kalnay et al. 1996) and are affected by input data as well as the assimilation system. Several studies have attempted to quantify uncertainties in the NRA air-sea fluxes (e.g. Hendon and Shinoda 1999, Smith et al. 2001). Comparison with research vessel measurements (Smith et al. 2001) show that NRA underestimates surface winds over most of tropics. Spatial and temporal characteristics of uncertainties of the NCEP reanalysis products in the IO are not well known. Our objective in this study is to examine how well NRA surface winds represent the seasonal cycle and intraseasonal variability in the IO relative to surface winds from QuikSCAT.

Scatterometers are spaceborne radars that infer surface winds from the roughness

of the sea surface. Wind speed and direction are inferred from measurement of microwave backscattered power from a given location on the sea surface at multiple antenna look angles. The SeaWinds scatterometer on the QuikSCAT satellite started operating in July 1999 and continues through the present. Measurement of radar backscatter from a given location on the sea surface are obtained from multiple azimuth angles as the satellite travels along its orbit. Estimate of vector winds are derived from these radar measurements over a single broad swath of 1600-km width centered around the satellite ground track. Scatterometer wind retrievals are calibrated to the neutral stability wind at a height of 10m above the sea surface (Chelton et al. 2001). We obtained the gridded QuikSCAT Level 3 data between July 19,1999 and December 31, 2001 at a resolution of 0.25^o x 0.25^o from the JPL SeaWinds Project. (http://podaac.jpl.nasa.gov/quikscat/). The Level 3 data have been created from the Direction Interval Retrieval with Threshold Nudging (DIRTH, Stiles 1999). Separate maps are provided for both ascending and descending pass. By maintaining the data at nearly the original sampling resolution and separating the ascending and descending passes, very little overlap occurs in one day. However, when overlap between subsequent swaths does occur, values are over written, not averaged. The data also contains several classes of rain flags indicating possible contamination of QuikSCAT observations based on rain estimates from three other satellites that are in operation simultaneously with QuikSCAT. We eliminated all rain flagged observations from the analysis. Observations from either ascending or descending passes in rain free regions are used to obtain daily maps. The daily maps still contain some gaps. For applications for which derivative products such as vorticity and divergence are important, the gaps need to be filled carefully using objective analysis technique (e.g. Pegion et al. 2000). We use a three day running mean at each grid box to obtain nearly complete spatial coverage. No spatial interpolation is used. Since we are primarily interested in studying the seasonal cycle and intraseasonal variability, some loss of kinetic energy on daily time scale due to three day running mean is acceptable. The three-day running mean wind product is referred to as QSCT winds in the text. The superior sampling of the QuikSCAT satellite compared to previous scatterometers is discussed in detail by Schlax et al. (2001). Chelton et al. (2001) carried out a comparison of 3-day mean QSCT wind speed with 3-day mean wind speed measured from the eastern Pacific TAO buoys with the 3-month data from 21 July to 20 October, 1999. The mean difference and rms error (rmse) from about 1700 collocated observations were found to be 0.74 m s^{-1} (TAO higher than QSCT) and 0.71 m s^{-1} respectively. The differences are partially due to sampling differences between TAO and QSCT.

The deep sea moored buoys, located in the Bay of Bengal and eastern Arabian Sea, of the National Data Buoy program (NDBP) of DOD measure several near surface meteorological and oceanic variables (Rao and Premkumar 1998) including wind speed and direction at 3 m height every three hours. Each three-hourly wind observation is a 10-minute average wind speed and direction sampled at 1Hz by a cup anemometer with vane (make: Lambrecht). The stated accuracy of wind speed measurements is 1.5% of full scale (0-60 m s^{-1}), i.e. 0.9 m s^{-1}. The three hourly data were averaged to obtain daily winds. The data from the deep sea buoys, although intermittent have proved to be useful

in validating reanalysis and satellite products over the north IO (Sengupta et al. 1999, Senan et al. 2001). Buoy data have also been useful in identifying important intraseasonal oscillations in sea surface temperature (SST) and surface heat fluxes in the Bay of Bengal (Sengupta and Ravichandran, 2001, Sengupta et al. 2001). Based on the longest available record with minimum gaps, we use surface wind data from two buoys, one each in the Bay of Bengal and the Arabian Sea. The Arabian Sea buoy (DS1) is located at 15.5°N, 69.25°E throughout the period (July 1999 to December 2001) while the Bay of Bengal buoy was located at 13°N, 87°E during 1999 but was moved to 12.15°N, 90.75°E at the beginning of 2000. The buoy winds at 3m height are extrapolated to 10m height using a power law (Panofsky and Dutton 1984). No attempt has been made to correct the buoy winds for near surface stability of the atmosphere.

Finally, to understand the differences between the NRA and QSCT winds, we make use of NRA precipitation as well as pentad precipitation analyses from the Climate Prediction Center Merged Analysis of Precipitation (CMAP). The CMAP pentad analysis uses the same algorithm and data sources as the monthly analysis of Xie and Arkin (1994), and is based on a blend of rain gauge data and five different satellite estimates of precipitation using infrared and microwave sensors.

3. Results

We compare the NRA and QSCT wind speed with in situ measurements from moored buoys at DS1 and DS3. Since the QSCT winds we use are 3-day running mean winds, a 3-day running mean was applied to buoy data as well as to NRA data. The buoy data is not continuous at either location. Between October 1, 1999 and July 31, 2001, there is a total of 374 days of data at DS1 and 405 days of data at DS3. Because the length of data from the buoys is rather limited, we carry out a simple comparison of QSCAT and NRA winds with buoy winds. QSCT and NRA winds at their original grid points nearest to the location of DS1 and DS3 were extracted and scatterplots of QSCT and buoy and of NRA and buoy zonal and meridional winds at DS1 and DS3 are shown separately in Fig.1. The rms differences and correlation are shown in each panel. The mean rms difference over the buoy locations between QSCT and buoy zonal and meridional winds are 1.42 m s^{-1} and 1.40 m s^{-1} respectively while those between NRA and buoy are 2.05 m s^{-1} and 2.04 m s^{-1} respectively . Thus, QSCT appears to represent the observed surface winds better than NRA. The least square linear fit is also plotted in each panel. We note that rms difference between QSCT and the limited in situ observations over the Bay of Bengal and Arabian Sea is larger than that found by Chelton et al. (2001) over the eastern Pacific.

3.1 The Annual Cycle

In this section, we compare the annual cycle of surface winds in NRA with that of QSCT. As the two products are on two quite different horizontal grids, they are re-gridded to a 1.5° x 1.5° latitude-longitude grid to facilitate quantitative comparison. Box averaging is used to go from a 0.25° x 0.25° grid to a 1.5° x 1.5° grid in the case of QSCT data while a 4-point Bessel interpolation is used to go from the T62 Gaussian grid (1.875°

x approximately 1.92^o) grid to a 1.5^o x 1.5^o grid for NRA. The annual cycle of QSCT wind vectors and wind speed is shown in Fig. 2. Mean winds are averages over corresponding months of 2000 and 2001. In addition to winter (Jan-Feb) and summer (Jul-Aug), we show spring (Apr-May) and fall (Oct-Nov) winds to illustrate that the mean zonal winds in the equatorial IO east of 50^{o}E are westerly during these two periods of the year. Averaged over July and August, the maximum wind speed in the Somali jet is about 13 m s^{-1} at approximately 59^{o}E and 12^{o}N. The differences between NRA and QSCT (NRA-QSCT) zonal (U) and meridional (V) winds averaged over December-January-February (DJF) and June-September (JJAS) are shown in Fig.3. Major differences in zonal winds occur only in the equatorial IO east of 60^o E. The largest differences are seen in the eastern equatorial IO where NRA eastward zonal winds can be upto 2ms^{-1} smaller than QSCT. This represents a substantial difference as the mean zonal wind in this region is only 2-4 m s^{-1} (Fig.2). We also note that the monsoon westerlies are generally weaker in NRA compared to QSCT during JJAS. The meridional winds are generally weaker in NRA than in QSCT south of the equator by 1.0-1.5 m s^{-1} during both the seasons. The cross-equatorial flow in the western equatorial IO and the southerlies in the Somali jet region are 1-2 m s^{-1} weaker in NRA than in QSCT during JJAS, but are 1.0-1.5 m s^{-1} stronger during DJF. The differences in both U and V during JJAS show that the large-scale summer monsoon flow is generally weaker in NRA than in QSCT. Similarly, the differences in U and V during DJF also indicate that the northeast winter monsoon flow is also weaker in NRA than in QSCT.

Daily anomalies are needed to study the intraseasonal variability. As the annual cycle is rather strong in this region, daily anomalies have to constructed with respect to the annual cycle. Since the QSCT data is only two and a half years long, it is not possible to construct a daily climatology. In the absence of a long daily record, an annual cycle can be defined as the sum of annual mean and first three harmonics (360, 180 and 120 day periods) of data for each year. Average of the annual cycles of 2000 and 2001 provides approximate measure of the mean annual cycle. This method of constructing annual cycle has been found useful in defining daily and intraseasonal anomalies (Goswami et al. 1998, Goswami and Ajaya Mohan, 2001). Such annual cycles were constructed for both NRA and QSCT and their evolution was examined at several locations in the Bay of Bengal and in Arabian Sea (not shown). No significant phase difference is noted in the seasonal evolution of the two wind products. However, the amplitude of the annual cycle is significantly weaker in NRA zonal winds specially in the eastern equatorial IO (consistent with Fig.3).

One of the most spectacular features of the annual cycle in this region is the onset of the Indian Summer monsoon which is best characterized by the evolution of the kinetic energy (KE) of the low level flow in the Somali Jet region (Webster and Yang, 1992, Goswami, 1998). The onset of the Indian summer monsoon in the two products is examined through the daily KE averaged over 55^o E-65^o E, 10^o N-15^o N during 2000 and 2001 (Fig.4). The dynamical onset of the monsoon is characterized by increase in the KE by more than a factor of 10 in a span of about a week sometime in the middle or late May. The timing of onset of the Indian summer monsoon during the two years is identical in both products. However, the energy of the intraseasonal fluctuations during the

summer monsoon period is higher in QSCT than in NRA. This difference in representation of the intraseasonal oscillations in the two products is examined in greater detail in the next section.

3.2 Intraseasonal Variability

As described in the previous section, the annual cycle is constructed as a sum of the annual mean and the first three harmonics of daily data for each year. As data for a full one year is not available for QSCT winds during 1999, the annual cycle is constructed from the available data as the sum of the mean and first two harmonics. Daily anomalies are constructed by subtracting the annual cycle each year from each field. To get a measure of daily fluctuations of the winds, standard deviation (SD) of daily wind speed anomalies during winter (DJF) of 1999-2000 and 2000-2001 and summer (JJAS) of 2000 and 2001 were calculated for QSCT. The SD for the two years were averaged to get a mean SD. The mean SD of daily wind speed anomalies during DJF and JJAS for QSCT are shown in Fig.5a,b. Mean SD of NRA wind speed anomalies were also calculated for the two seasons and the ratios between SD of daily anomalies NRA and QSCT are shown in Fig.5c,d. The largest amplitude of daily anomalies is 2-3 m s^{-1} over the south equatorial IO and South China Sea in winter and eastern equatorial IO and western Pacific in summer. The amplitude of daily variations of wind speed in the equatorial IO and western Pacific in NRA is about 60%-80% of that in QSCT. Further examination (not shown) reveals that weaker fluctuations of wind speed in NRA in the equatorial region results primarily from weaker zonal wind fluctuations. Not only are the mean NRA zonal winds weaker compared to QSCT in the equatorial IO (Fig.3), the fluctuations of the zonal winds are also smaller. The correlation between daily anomalies of NRA and QSCT wind speed during winter and summer are shown in Fig.6. The correlation is poorest along most of the equatorial belt during summer while it is poorest in the eastern equatorial IO and eastern Arabian Sea during winter. The amplitude of daily anomalies in NRA are weaker and not in phase with QSCT anomalies over the equatorial IO.

To investigate how the NRA represents the amplitude of the intraseasonal component of the winds, both NRA and QSCT winds were passed through a 10-70 day Lanczos filter with 51 weights. As described above for the daily wind speed anomalies, the mean SD of the band-pass filtered anomalies from NRA and QSCT for the two seasons were calculated. Standard deviation of the NRA band-passed wind speed anomalies relative to those of QSCT band-passed wind speed anomalies during winter and summer are shown in Fig.7a, b. The ratio of SD of filtered wind speed anomalies (NRA/QSCT) shows that the intraseasonal variability of NRA wind speed is weaker than that of QSCT over most regions during both seasons. In particular, during summer over the equatorial IO east of 60^{o}E the amplitude of intraseasonal oscillation in NRA winds is only about 50% of that of QSCT winds. The ratio is between 0.9 and 1.1 in the central Bay, north Bay and central Arabian sea during northern summer. Thus, NRA seems to represent the summer monsoon intraseasonal variability in the Bay of Bengal and Arabian sea reasonably well. The temporal correlation between filtered wind speed anomalies from NRA and QSCT for the two seasons are shown in Fig.7c,d. Correlation at

each grid point for JJAS (DJF) was calculated by taking the two summers (winters) together. Correlation between the two products is poor (less than 0.5) over the equatorial IO during both seasons. The amplitude of inraseasonal oscillations in NRA winds are not only significantly weaker than those in QSCT, they are also out of phase with those in QSCT. We note (not shown) that during spring and fall too the amplitude of intraseasonal variability in NRA wind over the equatorial IO is significantly weaker than that of QSCT winds.

4. Discussions

Why are the mean as well as the intraseasonal variability in NRA surface winds over the equatorial IO systematically weaker than those in QSCT? Surface winds in the tropics are driven partly by deep tropospheric heating associated with tropical convection (Gill, 1980) and partly by surface pressure gradients associated with SST gradients (Lindzen and Nigam, 1987). Since seasonal mean SST gradients in the IO are rather weak, surface winds in this region are driven primarily by the elevated heating associated with tropical rainfall (Chiang et al. 2001). Therefore, the weakness in surface winds in NRA is likely to be related to the weakness in analysis of precipitation by NRA.

To test this hypothesis, we compare NRA precipitation analysis with observed precipitation, taking CMAP to represent observed precipitation. According to our hypothesis, the zonal winds in the central equatorial IO (say, between 70^{O}E and 95^{O}E) should be related to precipitation variations in the eastern IO (say, between 90^{O}E and 100^{O}E). This is indeed true in observation as seen in Fig.8a where CMAP precipitation (linearly interpolated to daily values) averaged over the eastern IO between 5^{O}N and 5^{O}S is plotted together with zonal winds averaged over the central IO during 2001. The correspondence between the two curves is evident. However, such a correspondence is missing in Fig.8b where NRA precipitation averaged over the eastern IO and NRA zonal winds in the central IO are plotted. We note that NRA precipitation in the eastern IO is rather weak and does not have significant intraseasonal oscillation. The intraseasonal oscillations in NRA zonal winds in the central IO are weaker than those in QSCT and appear to be unrelated to the eastern IO precipitation in NRA. The weakness in intraseasonal oscillation in NRA precipitation in the eastern IO is further illustrated in Fig.9 where we show precipitation averaged over the eastern IO box from CMAP and NRA during 2000 and 2001. Vigorous intraseasonal oscillation in precipitation with a period of about a month present in CMAP is missed by NRA most of the time. The mean precipitation in NRA in this region is only about one half of that in CMAP while the intraseasonal variance of precipitation in NRA is only about one third of that in CMAP. This seems to be the main reason why NRA underestimates the intraseasonal wind variability in equatorial IO.

Figure 9 shows that not only the intraseasonal variability but also the time mean precipitation over the eastern IO is much weaker in NRA compared to CMAP. To examine the spatial structure of this bias in NRA precipitation analysis, bi-monthly mean differences between NRA and CMAP precipitation are plotted in Fig.10. It is interesting to note that NRA significantly underestimates precipitation in the eastern equatorial IO and Indonesia and overestimates precipitation in the western equatorial IO. The

precipitation bias of 6-8 mm.day^{-1} is almost as large as the mean itself. The precipitation biases in the east and west IO are both likely to contribute to easterly wind bias in the central IO through biases in elevated heating. To test whether these biases in precipitation analysis may be related to the observed wind biases in NRA, we forced a linear model of surface winds (Saji and Goswami, 1996) by elevated heating corresponding to the mean precipitation bias corresponding to each month. The model of surface winds constructed by Saji and Goswami (1996) included the SST gradient effects in a Gill type model through a transformation as suggested by Neelin (1989). Our previous experiments with the model forced separately by SST and precipitation heating indicate that contribution of the observed SST gradients to the observed surface winds in this region is weak, contributing to less than a quarter of the observed wind magnitude. The influence of the SST gradients is, therefore, not included in the present simulations. Thus, the model is essentially a Gill (1980) model. As an example, the vector wind difference between NRA and QSCT averaged for January-February (JF) and October-November (ON) are shown in Fig.11a, b together with mean simulated vector winds (Fig.11c, d) forced by corresponding bimonthly mean precipitation bias (Fig.10). The good correspondence between the simulated winds and the wind bias over the oceanic regions indicates that the precipitation bias in the reanalysis is indeed responsible for a systematic underestimation of zonal winds by NRA in the equatorial IO, especially east of 60^{o}E. Improvement in NRA surface winds will therefore require improvement in NRA precipitation which depends on the physics of the forecast model used in the GDAS.

5. Summary and Conclusion

Reanalysis surface wind products such as NRA are very useful for studying ocean variability and large scale air-sea interactions as they provide long records of homogeneous 'data' with good spatial and temporal coverage. However, these products are significantly influenced by the atmospheric model used for assimilation. In this note, we examine the ability of the NRA surface winds to represent the observed annual cycle and intraseasonal variability over the IO. The scatterometer on the NASA satellite QuikSCAT provides surface wind speed and direction over the oceans with high horizontal and temporal resolution. Based on earlier studies of validation of QuikSCAT winds, we treat QuikSCAT winds as representative of in situ data, and compare NRA winds with them. During northern summer, the large scale monsoon flow is weaker in NRA than in QSCT. It is shown that the mean NRA zonal winds are approximately 2-3 m s^{-1} weaker than QSCT zonal winds in the equatorial IO. The NRA meridional winds, on the other hand, are slightly stronger than those from QSCT in the northern IO and 1-2 m s^{-1} weaker than QSCT in the southern IO. Our findings are consistent with those of Smith et al. (2001) who compared NRA products with research vessel measurements during the World Ocean Circulation Experiment (WOCE) for the period 1990-1995 and concluded that the NRA near surface wind speed is significantly underestimated at all latitudes. In addition to the bias, the daily variability is underestimated by NRA over large parts of the IO, specially over the equatorial IO where it is about 70% of the observed variability. Further analysis indicates that this essentially arises due to underestimation by NRA of

the intraseasonal variability of the wind. The amplitude of NRA intrasesaonal wind variations over the equatorial IO east of 60^{o}E is only about 50% of the amplitude in QSCT. It is shown that the NRA severely underestimates the mean as well as the intraseasonal variability of observed precipitation in the eastern IO. We show that NRA precipitation has a large negative bias in the eastern IO and a positive bias in the western IO. Using a simple model, it is shown that the bias in the NRA winds is related to the bias in NRA precipitation. It is further shown that the NRA underestimates the observed intraseasonal variability of precipitation in the eastern IO. The weaker than observed intraseasonal variability of NRA winds in the equatorial IO is also likely to be related to the weaker than observed intraseasonal variability of precipitation in the east in NRA.

An ocean model forced with the daily wind stress from NRA is, therefore, expected to simulate weaker inraseasonal Kelvin waves and weaker equatorial jets in the IO. Both these processes could significantly influence the intraseasonal as well as the seasonal variability in a model of IO. Latent heat fluxes estimated from NRA winds would also be generally underestimated, and this could affect the SST in the ocean model.

Acknowledgments: This work is partially supported by a grant from the Department of Ocean Development, New Delhi. We thank Retish Senan , D.S. Anitha, Prince Xavier and R. Vinay for help in analyzing the data.

References

Chelton, D. B., S.K. Esbensen, M.G. Schlax, N. Thum and M.H. Freilich, Observations of coupling between surface wind stress and sea surface temperature in the eastern tropical Pacific, *J. Climate, 14*, 1479-1498, 2001.

Chelton, D. B., Satterometer based assessment of surface wind field analysis from the European Center for Medium Range Weather Forecasts. In *Proc. WCRP/SCOR Workshop on Intercomparison and Validation of Ocean-Atmosphere Flux Fields.* May 21-24, MD. U.S.A. 2001.

Chiang, J.C.H., S.E. Zebiak and M.A. Cane, Relative roles of elevated heating and surface temperature gradients in driving anomalous surface winds over the tropical oceans. *J. Atmos. Sci. 58*, 1371-1394. 2001.

da Silva , A. M., C.C. Yong and S. Levitus, *Algorithms and Proceedure, Vol.1: Atlas of Marine Surface Data 1994*. NOAA Atlas NESDIS 6. 1994.

Gadgil, S. and S. Surendran : Monsoon precipitation in the AMIP runs, *Climate Dynamics, 14*, 659-689, 1998.

Gibson, J.K., P. Kalberg, S. Uppala, A. Hernandez, A. Namura and E. Serano, ERA description, *ERA project report series.* ECMWF, Reading. 1997.

Gill, A., Some simple solutions for heat induced tropical circulation. *Quart. J. Roy. Meteorl. Soc. 106*, 447, 462. 1980.

Goswami, B.N., Inter-annual variation of Indian summer monsoon in a GCM: External conditions versus internal feedbacks. *J. Climate, 11*, 501-522. 1998.

Goswami, B.N. , D. Sengupta and G. Suresh Kumar, intraseasonal Oscillations and Inter-annual variability of surface winds over the Indian monsoon region. *Proc. Indian Aca. Sci. (Earth & Panet. Sci) 107*, 45-64. 1998.

Goswami, B.N. And R.S. Ajaya Mohan, Intra-seaonal oscillations and inter-annual variability of the Indian summer monsoon. *J. Climate, 14*, 1180-1198. 2001.

Han, W., J.P. McCreary, D.L.T. Anderson, A.J. Mariano, Dynamics of the eastern surface jets in the equatorial Indian Ocean. *J. Phys. Oceanog. 29*, 2191-2209. 1999.

Han, W., D. M. Lawrence and P.J. Webster, Dynamical response of equatorial Indian Ocean to intraseasonal winds: zonal flow. *Geophy. Res. Letts. 28*, 4215-4218, 2001.

Hendon, H. T. Shinoda, Assessment of warm pool surface fluxes form NCEP reanalysis. *COARE-98 Conf. Proc. TOGA Coupled Ocean Atmosphere Response Experiment (COARE)* , Boulder, CO. 7-14 July, 1998. WCRP-107, WMO/TD-940, WMO, Geneva, 255pp.1999.

Kalnay, E., M. Kanamitsu, R. Kistler, W. Collins, D. Deaven, L. Gandin, M. Iredell, S. Saha, G. While, J. Woolen, Y. Zhu, M. Chelliah, W. Ebisuzaki, W. Higgins, J. Janowiak, K. C. Mo, C. Ropelewski, J. Wang, A. Leetma, R. Reynolds, Roy Jenne and Denis Joseph, The NCEP/NCAR reanalysis project. *Bull. Am. Meteorol. Soc. 77*, 437-471, 1996.

Lindzen, R.S. And S. Nigam, On the role of sea surface temperature gradients in forcing low level winds and convergence in the tropics. *J. Atmos. Sci. 44*, 2418-2436,

1987.

Liu W. T., Progress in scatterometer application, *J. Oceanography, 58*, 121-136, 2002.

McCreary, J. P., P. K. Kundu and R.L. Molinari, A numerical investigation of dynamics, thermodynamics and mixed layer processes in the Indian Ocean. *Progress in Oceanography. Vol.31*, Pergamon, 181-224,1993.

McPhaden, M. J., Variability in the central equatorial Indian Ocean, Part II: Oceanic heat and turbulent energy balances. J. Mar. Res. 40(2), 403-419,1982.

Murtugudde, R., R. Seager and A.J. Busalacchi, Simulation of tropical oceans with an ocean GCM coupled to an atmospheric mixed layer model. *J. Climate*, 9, 1795-1815, 1998.

Murtugudde, R.,and A.J. Busalacchi, Inter-annual variability of the dynamics and thermodynamics of the tropical Indian Ocean. *J. Climate, 12*, 2300-2326,1999.

Murtugudde, R., J.P. McCreary Jr. and A.J. Busalacchi, Oceanic processes associated with anomalous events in the Indian Ocean with relevance to 1997-1998. *J. Geophy. Res. , 105*, 3295-3306, 2000.

Naderi, F. M., M. H. Freilich, and D. G. Long, Spaceborne radar measurements of wind velocity over the ocean- An overview of NSCAT scatterometer system. P*roc. IEEE, 79*, 850-866, 1991.

Neelin, J. D. On the interpretation of the Gill model. J. *Atmos. Sci. 46*, 2466-2468. 1989.

Panofsky, H. A. and J. A. Dutton, *Atmospheric Turbulence*, John Weily and Sons, New York, 397pp. 1984.

Pegion, P.J., M. A. Bourassa, D.M. Legler, and J.J. O'Brien, Objectively derived daily winds from satellite scatterometer data. *Mon. Wea. Rev. 128*, 3150-3168, 2000.

Rao, Y.R and K. Premkumar, A preliminary analysis of meteorological and oceanographic observations during the passage of a tropical cyclone in Bay of Bengal. NIOT technical note, NIOT-NDBP-TR-001/98, 1998.

Saji, N.H. And B.N. Goswami : An improved linear model of tropical surface wind variability. *Quart. J. Roy. Meteorl. Soc. 122*, 23-53. 1996.

Saji, N.H. and B.N. Goswami, An inter-comparison of the seasonal cycle of tropical surface stress simulated by 17 GCMs. *Climate Dynamics. 13*, 561-585. 1997.

Saji, N. H. , B. N. Goswami, P. N. Vinaychandran and T. Yamagata, A dipole mode in the tropical Indian Ocean. *Nature, 401*, 360-363. 1999.

Schiller, A, J.S. Godfrey, P.C. McIntosh,G. Meyers and R. Fiedler, Inter-annual dynamics and thermodynamics of the Indo-Pacific Oceans. J. Phys. Ocean. 30, 987,1012, 2000.

Senan R., D.S. Anitha and D. Sengupta , Validation of SST and wind speed from TRMM using north Indian Ocean moored buoy observations. *CAOS Report 2001AS1*, Centre for Atmospheric Sciences, Indian Institute of Science, Bangalore-560 012. India, 2001.

Sengupta, D., P. Joseph, R. Senan and G. Suresh Kumar , Validation NCEP daily surface winds over the north Indian Ocean. *CAOS Report 99AS1*, Centre for Atmospheric Sciences, Indian Institute of Science, Bangalore-560 012. India, 1999.

Sengupta, D. and M. Ravichandran, Oscillations of Bay of Bengal sea surface temperature during the 1998 summer monsoon. *Geopgys. Res. Letts. 28*, 2033-

2036, 2001.

Sengupta, D., B.N. Goswami, R. Senan, Coherent intraseasonal oscillations of ocean and atmosphere during Asian Summer monsoon. *Geophys. Res. Letts. 28*, 4127-4130, 2001.

Smith, S. R., D. M. Legler and K.V. Verzone, Quantifying uncertainties in NCEP reanalyses using high quality research vessel observations. *J. Climate, 14*, 4062-4072. 2001.

Schlax M.G., D.B. Chelton and M.H. Freilich, Sampling errors in wind fields constructed from single and tandem scatterometer datasets. *J. Atmos. Ocean. Tech. 18*, 1014-1036, 2001.

Stiles B. W., *Special Wind Vector Data Product: Direction Interval Retrieval with Threshold Nudging (DIRTH) Product Description, Version 1.1*. Jet Propulsion Laboratory, Pasadena, CA, U.S.A. 1999.

Vinayachandran, P. N. , S.R. Shetye, D. Sengupta and S. Gadgil, Forcing mechanisms of the Bay of Bengal Circulation. *Current Science*, *71*, 753-763. 1996.

Webster, P.J. And S. Yang, Monsoon and ENSO: Selectively interactive systems. *Quart. J. Roy. Meteorl. Soc. 118*, 877, 926, 1992.

Webster, P.J., V. O. Magana, T. N. Palmer, J. Shukla, R. A. Tomas, M. Yanai and T. Yasunari, Monsoons: Processes, predictability and the prospects for prediction. *J. Geophys. Res. 103,C7*, 14,451-14,510. 1998.

Wyrtki, K., An equatorial jet in the Indian Ocean, *Science, 181*, 262-264, 1973.

Xie P.P. and P.A. Arkin Analysis of global monthly precipitation using gauge, satellite observations and numerical model precipitation. *J. Climate*, *9*, 840-858, 1996.

Figure Legends

Figure 1: Scatter plot between zonal (U) and meridional (V) winds (m s^{-1}) from QSCT and Buoys, DS1 upper four panels) and DS3 (lower four panels). The rms difference (m s^{-1}) and correlation between the variables are shown in each panel. The straight line represents least square linear fit with slope m and intercept c.

Figure 2: Bimonthly mean wind vectors and isotachs (m s^{-1}) from QSCT for January-February (JF), April-May (AM), July-August (AG) and October-November (ON). Isotachs greater than 6 m s^{-1} are shaded.

Figure 3: Mean zonal wind (U) differences (m s^{-1}) between NRA and QSCT (NRA-QSCT) for DJF and JJAS (upper panels). Mean meridional wind (V) differences are in lower panels.

Figure 4: Evolution of daily kinetic energy (m^2s^{-2}) for 2000 and 2001 averaged over a box (55^oE-65^oE, 10^oN-15^oN) in the Somali jet region. NRA (solid), QSCT (dashed).

Figure 5: Standard deviation (SD) of daily wind speed anomalies in QSCT during winter , DJF (a) and summer, JJAS (c) and ratio of SD of NRA and QSCT anomalies (b,d). S.D values less than $2ms^{-1}$ are shaded while SD ratio less than 1.0 are shaded. Anomalies for two winter (1999/2000 and 2000/2001) and summer (2000 and 2001) seasons are used in calculating the mean SD.

Figure 6: Temporal correlation between daily wind speed anomalies of NRA and QSCT during winter (DJF) and summer (JJAS). Anomalies for two winter (1999/2000 and 2000/2001) and summer seasons (2000 and 2001) are used in calculating the mean correlation. Correlation greater than 0.5 are shaded.

Figure 7: Ratio of standard deviation (a,b) and correlation of 10-70 day filtered NRA and QSCT wind speed anomalies for winter (DJF) and summer (b, JJAS). Anomalies for two winter (1999/2000 and 2000/2001) and summer (2000 and 2001) seasons are used in calculating the mean SD and correlation.

Figure 8: (a) Time series of precipitation anomalies (mm.day^{-1}) averaged over 90^oE-100^oE and 5^oS-5^oN from CMAP for 2001 (solid) zonal wind anomalies (m s^{-1}) averaged over 70^oE-95^oE and 5^oS-5^oN from QSCT (dashed). (b) Same as in the top panel but for NRA precipitation (solid) and NRA zonal winds (dashed)

Figure 9: Time series of precipitation anomalies (mm.day^{-1}) averaged over 90^oE-100^oE and 5^oS-5^oN from CMAP and NRA for (a) 2000 and (b) 2001. Pentad CMAP anomalies were linearly interpolated to daily values. Mean and variance each time series are indicated.

Figure 10: Bimonthly mean bias (NRA-CMAP) of analyzed precipitation (mm/day) of NRA compared to observations (CMAP). Negative contours are shaded. Two years of data from 2000 and 2001 are used to create the mean.

Figure 11: (a,b) Bimonthly mean vector wind difference (m s^{-1}) and isotachs between NRA and QSCT for January-February (JF) and October-November (ON). (c,d) Bimonthly mean vector wind anomalies (m s^{-1}) and isotachs for JF and ON simulated by a linear model forced by corresponding bimonthly mean precipitation biases in NRA as shown in Fig.10.

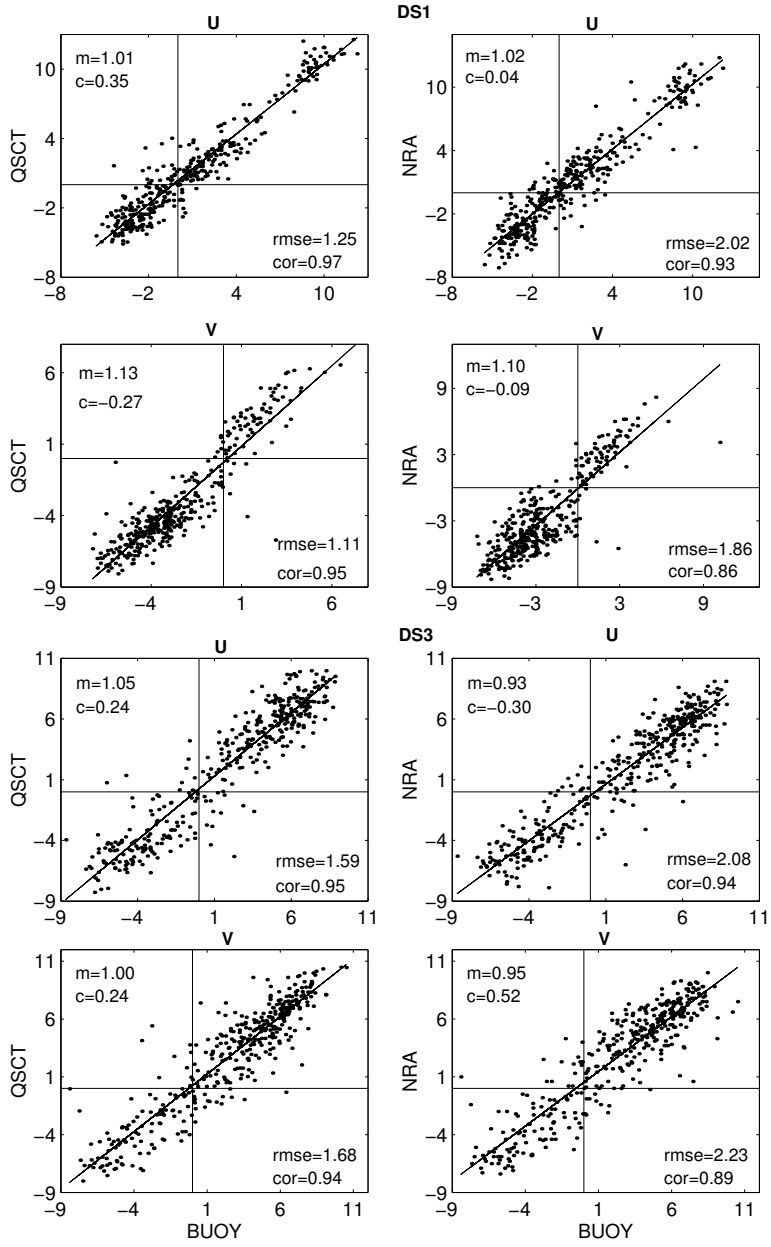

Figure 1: Scatter plot between zonal (U) and meridional (V) winds (ms^{-1}) from QSCT and Buoys, DS1 (upper four panels) and DS3 (lower four panels). The rms difference (ms^{-1}) and correlation between the variables are shown in each panel. The straight line represents least square linear fit with slope m and intercept c.

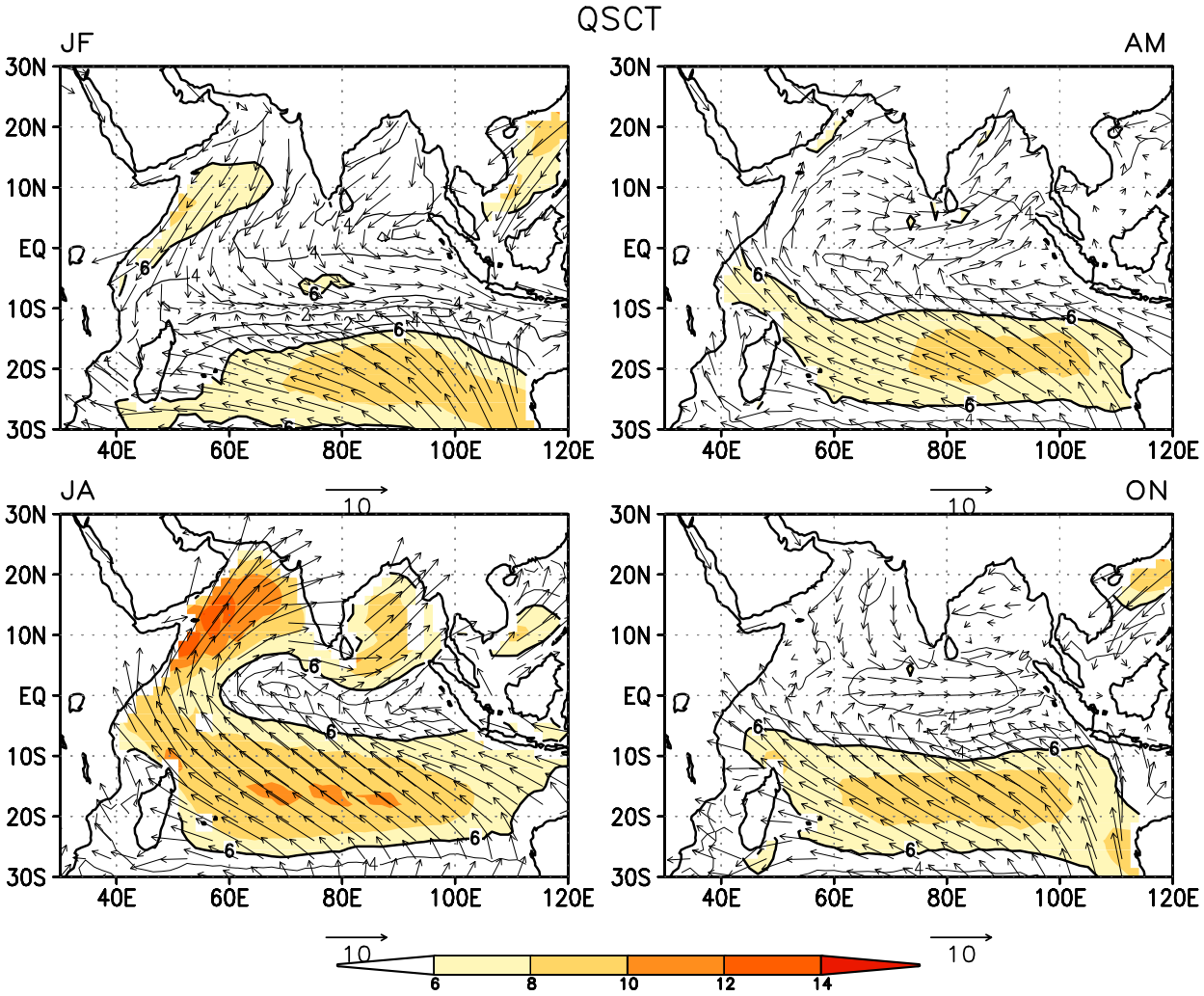

Figure 2: Bimonthly mean wind vectors and isotachs (ms^{-1}) from QSCT for January-February (JF), April-May (AM), July-August (AG) and October-November (ON). Isotachs greater than 6 ms^{-1} are shaded.

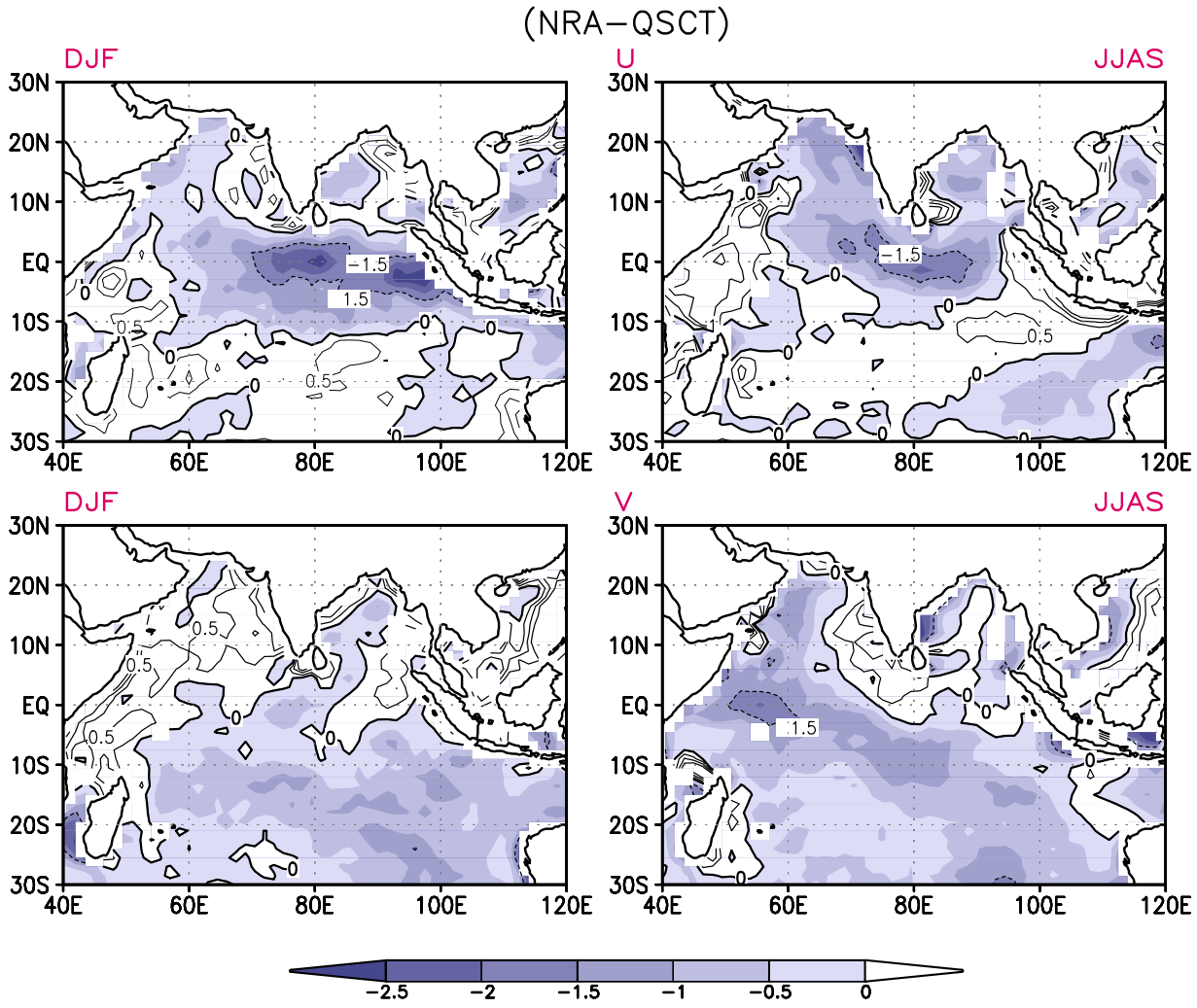

Figure 3: Mean zonal wind (U) differences (ms^{-1}) between NRA and QSCT (NRA-QSCT) for DJF and JJAS (upper panels). Mean meridional wind (V) differences are in lower panels.

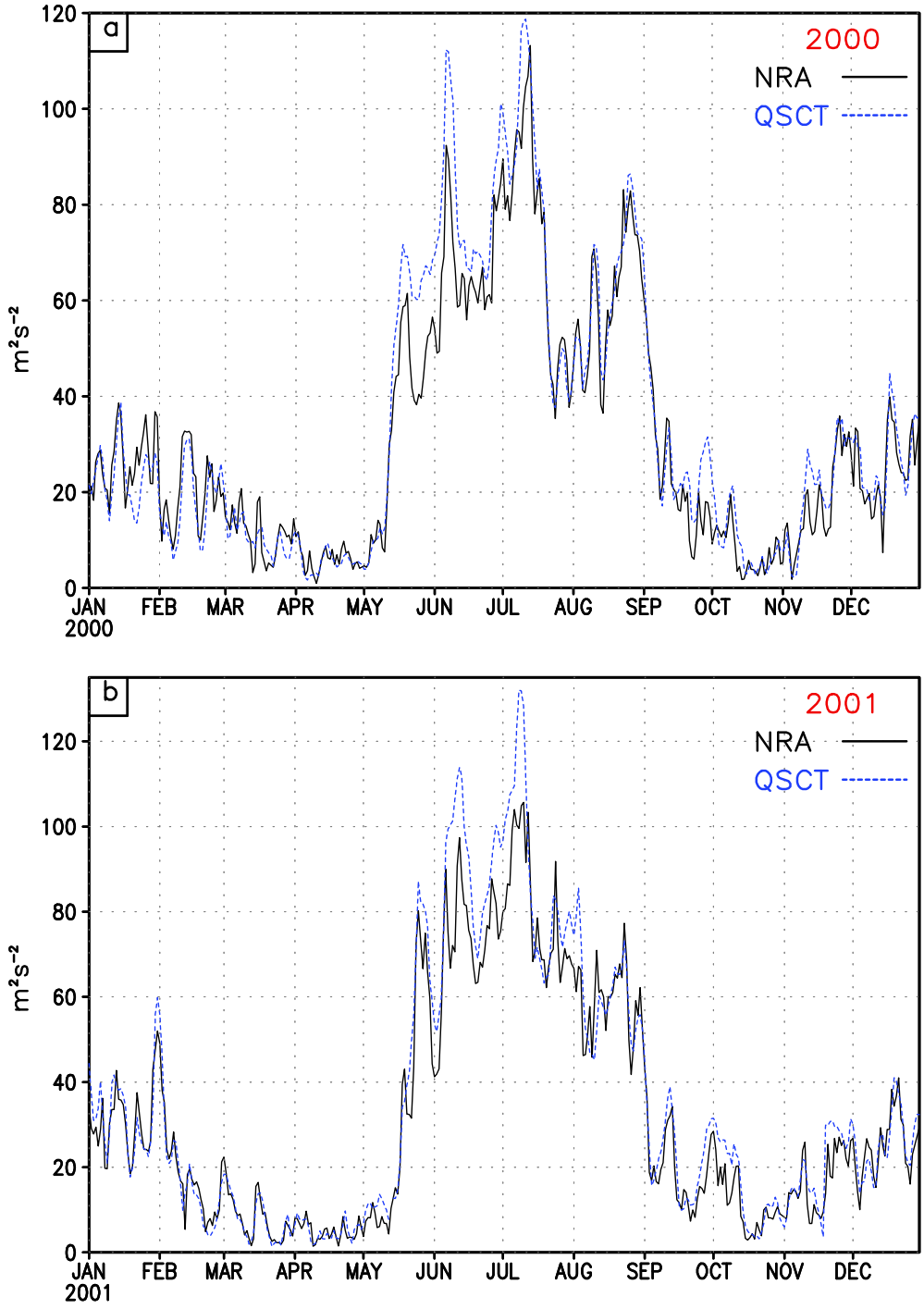

Figure 4: Evolution of daily kinetic energy ($m^2 s^{-2}$) for 2000 and 2001 averaged over a box (55°E-65°E, 10°N-15°N) in the Somali jet region. NRA (solid), QSCT (dashed).

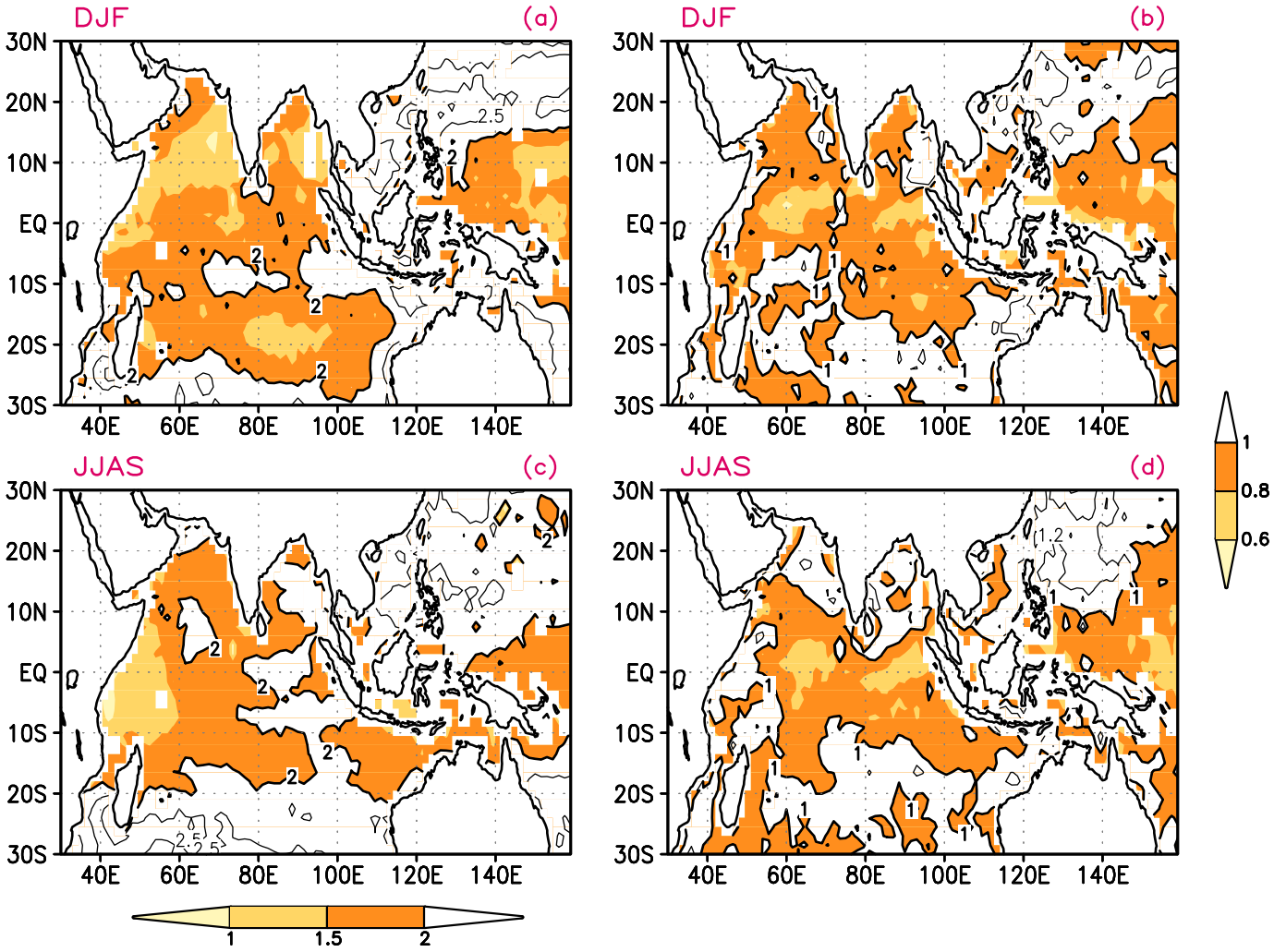

Figure 5: Standard deviation (SD) of daily wind speed anomalies in QSCT during winter , DJF (a) and summer, JJAS (c) and ratio of SD of NRA and QSCT anomalies (b,d). S.D values less than $2ms^{-1}$ are shaded while SD ratio less than 1.0 are shaded. Anomalies for two winter (1999/2000 and 2000/2001) and summer (2000 and 2001) seasons are used in calculating the mean SD.

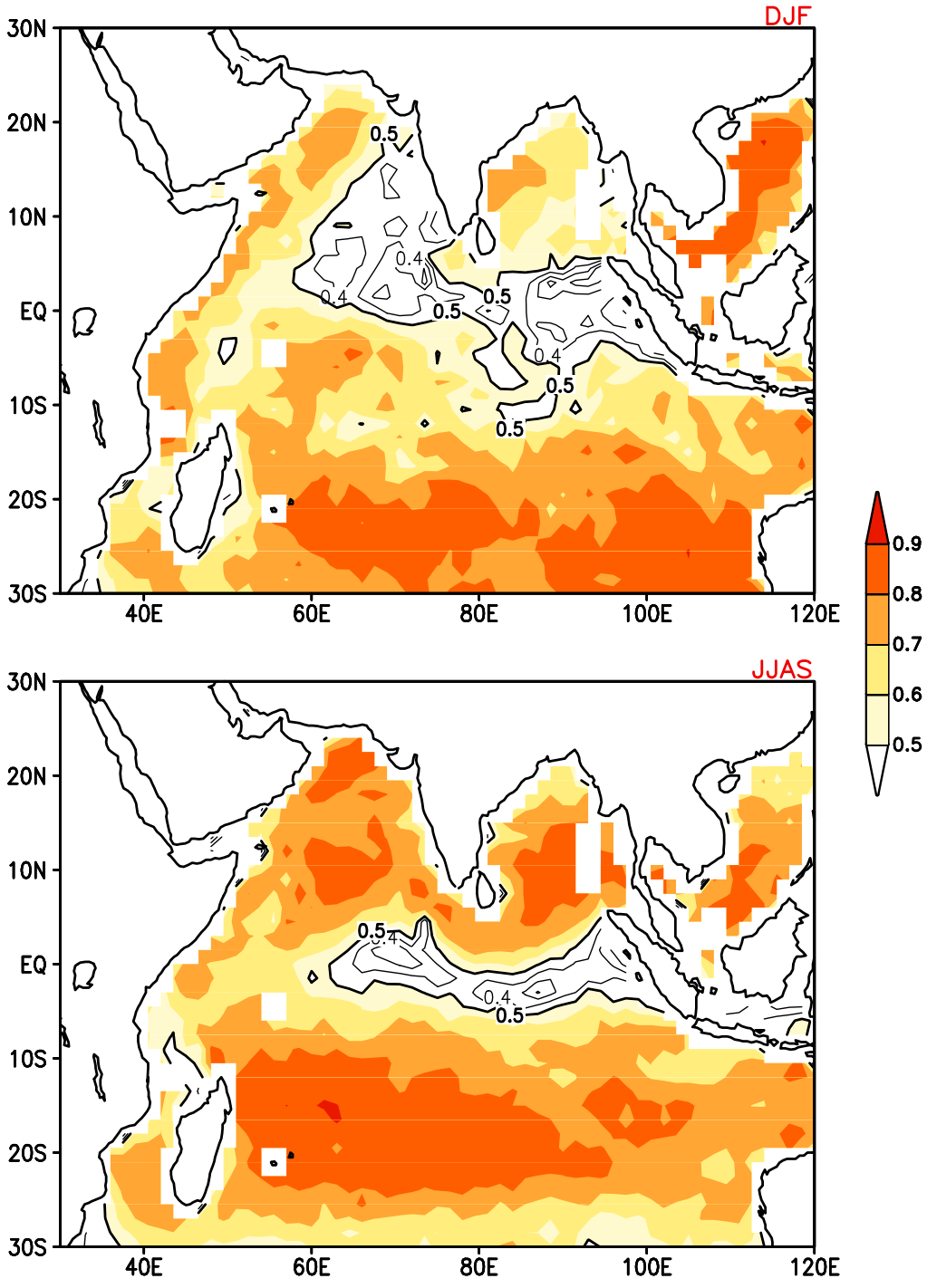

Figure 6: Temporal correlation between daily wind speed anomalies of NRA and QSCT during winter (DJF) and summer (JJAS). Anomalies for two winter (1999/2000 and 2000/2001) and summer seasons (2000 and 2001) are used in calculating the mean correlation. Correlation greater than 0.5 are shaded.

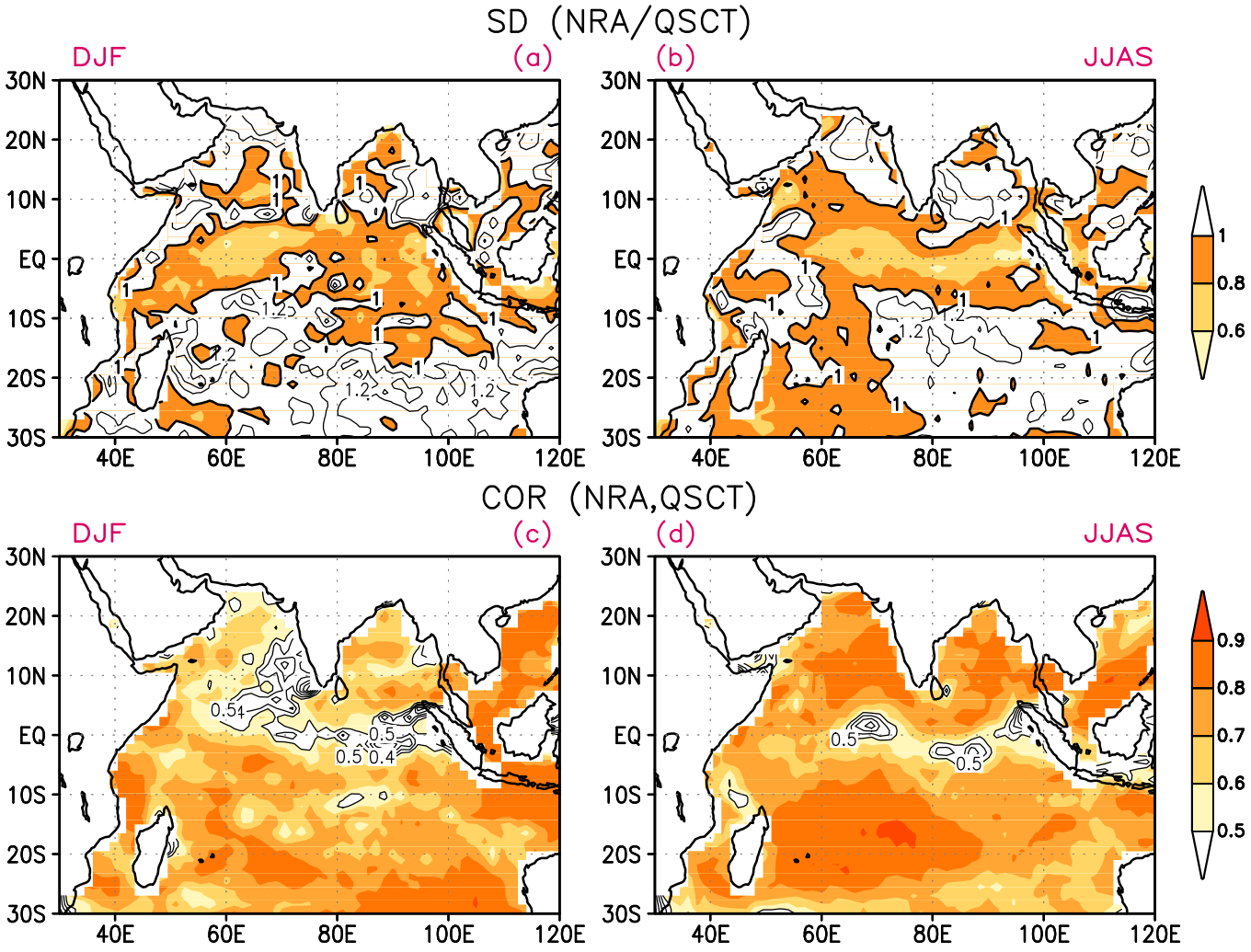

Figure 7: Ratio of standard deviation (a,b) and correlation of 10-70 day filtered NRA and QSCT wind speed anomalies for winter (DJF) and summer (b, JJAS). Anomalies for two winter (1999/2000 and 2000/2001) and summer (2000 and 2001) seasons are used in calculating the mean SD and correlation.

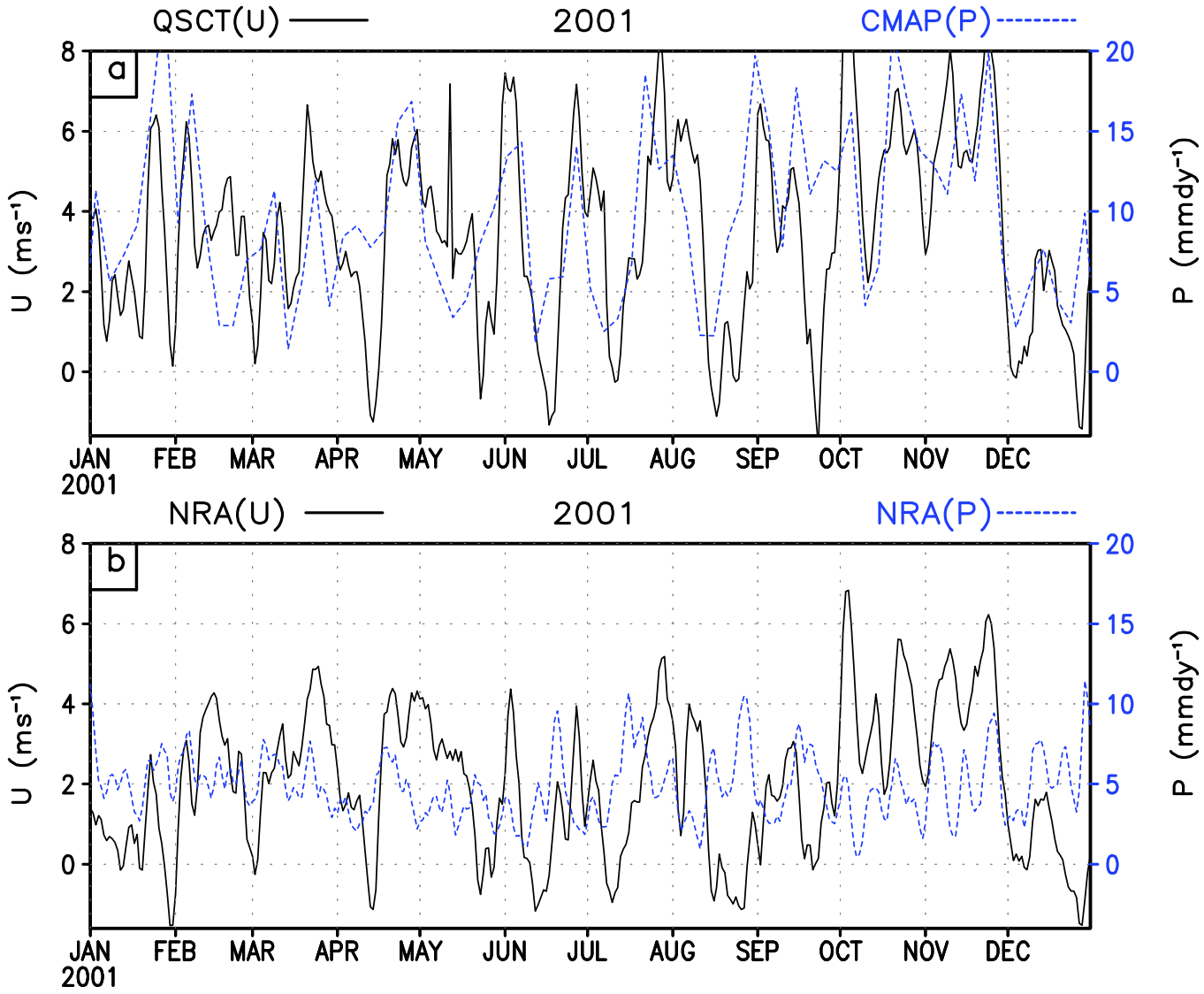

Figure 8: (a) Time series of precipitation anomalies ($mm.day^{-1}$) averaged over 90°E-100°E and 5°S-5°N from CMAP for 2001 (solid) zonal wind anomalies (ms^{-1}) averaged over 70°E-95°E and 5°S-5°N from QSCT (dashed). (b) Same as in the top panel but for NRA precipitation (solid) and NRA zonal winds (dashed)

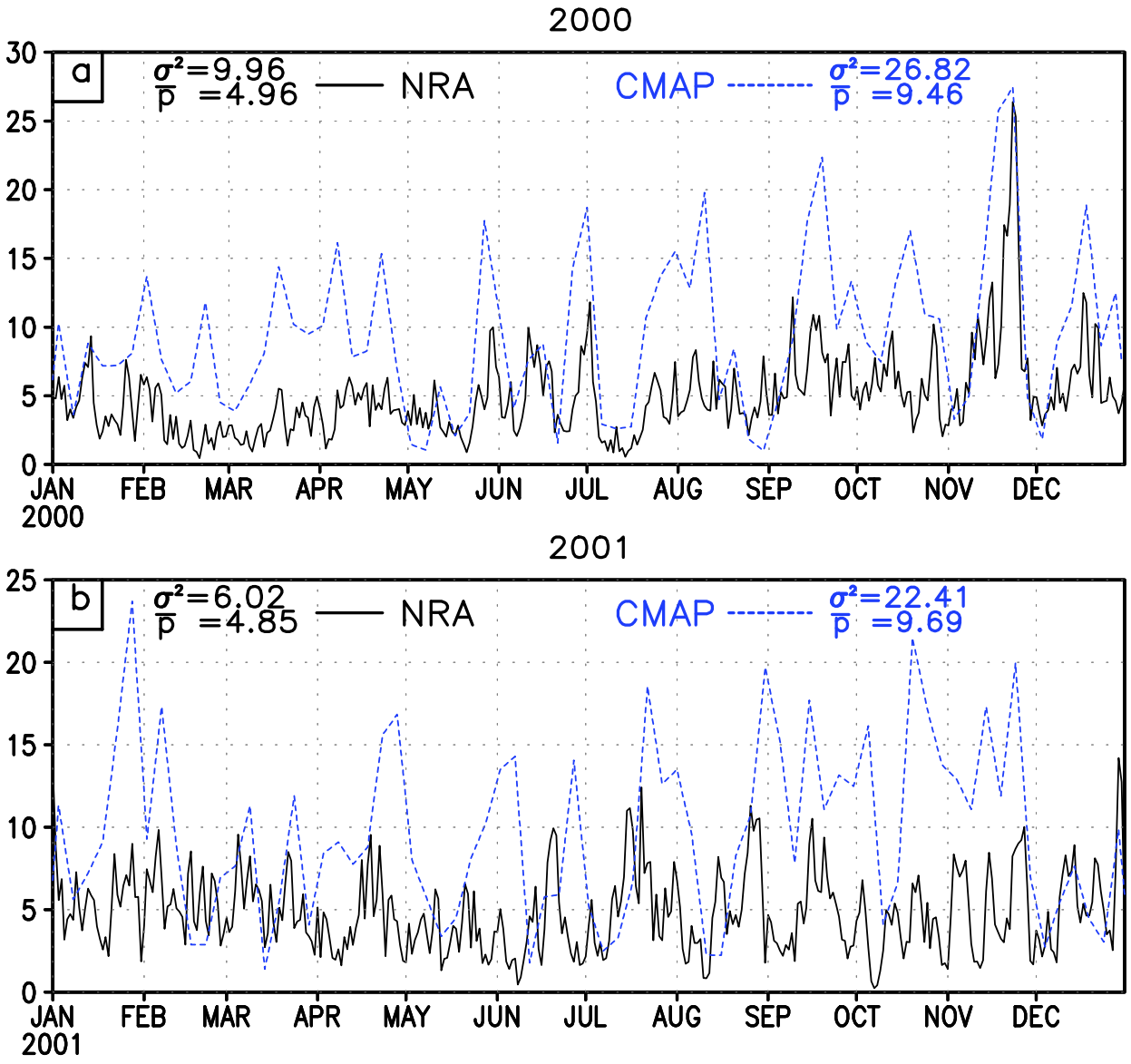

Figure 9: Time series of precipitation anomalies ($mm.day^{-1}$) averaged over 90°E-100°E and 5°S-5°N from CMAP and NRA for (a) 2000 and (b) 2001. Pentad CMAP anomalies were linearly interpolated to daily values. Mean and variance each time series are indicated.

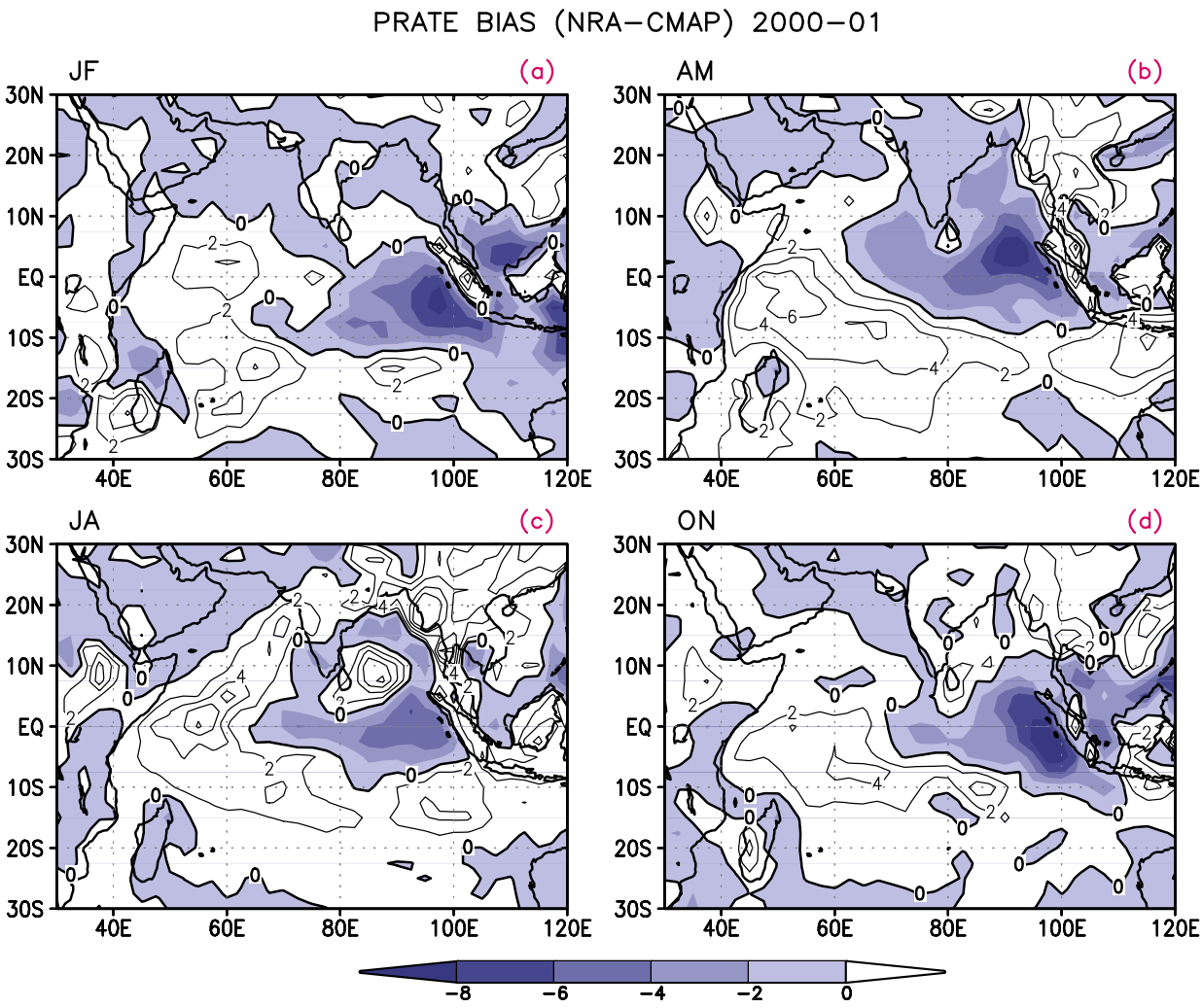

Figure 10: Bimonthly mean bias (NRA-CMAP) of analyzed precipitation (mm/day) of NRA compared to observations (CMAP). Negative contours are shaded. Two years of data from 2000 and 2001 are used to create the mean.

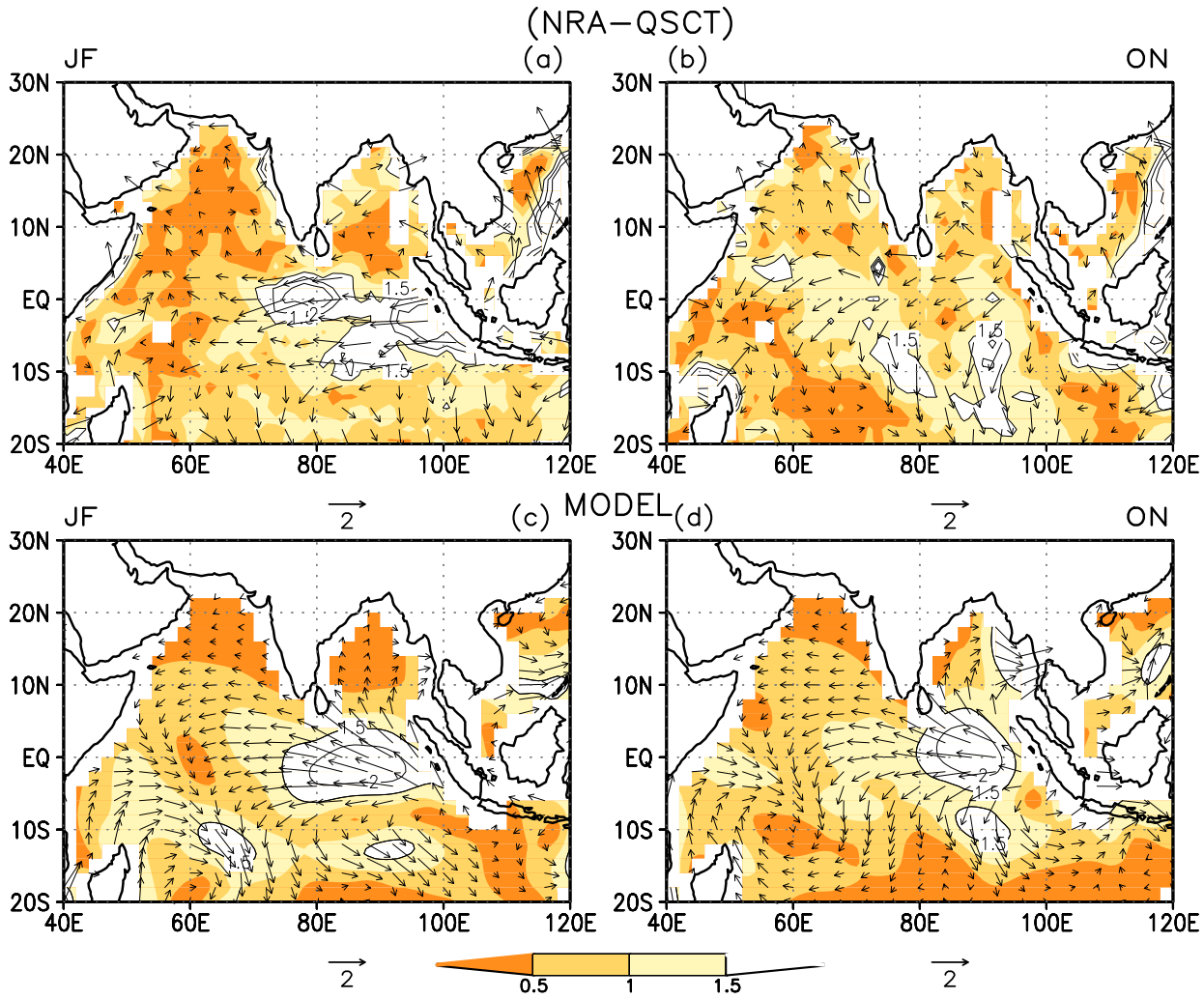

Figure 11: (a,b) Bimonthly mean vector wind difference (ms^{-1}) and isotachs between NRA and QSCT for January-February (JF) and October-November (ON). (c,d) Bimonthly mean vector wind anomalies (ms^{-1}) and isotachs for JF and ON simulated by a linear model forced by corresponding bimonthly mean precipitation biases in NRA as shown in Fig.10.